ABSTRACT

ROLE OF CATALYST AND SUBSTRATE IN SYNTHESIS OF SINGLE WALL CARBON NANOTUBES

by
Amit Goyal

The synthesis of single wall carbon nanotubes (SWNTs) by the catalytic disproportionation of carbon monoxide (CO) (i.e., Boudouard reaction) at 1 atm pressure and 700-800 C, has been systematically investigated in order to determine whether the process can be used for the large scale production. SWNT diameter distribution and morphology were studied by Raman scattering, and scanning and transmission electron microscopy, respectively. X-ray diffraction was used to determine levels of the remnant catalyst and support. Synthesis experiments were conducted using a three-stage process with hydrogen to reduce the catalyst-precursor and argon to cool the system. Two types of catalyst/support synthesis were studied: (1) Combustion synthesis to form catalyst on high surface area MgO support, and (2) Tetraethoxysilane synthesis to form catalyst on arrayed 200 nm silica opal support. Cobalt to molybdenum atomic weight ratios of 1:4 and 5:1 respectively were found to be most effective for the selective production of SWNTs, and by contrast with previous observations in the literature, cobalt alone as catalyst was also found to be very effective under these synthesis conditions. Molybdenum alone is not active, but having some Mo in combination with Co increases SWNT yields. This suggests that Mo plays the role of a promoter by preventing the segregation of the active Co particles. MgO support could be easily removed using 4 M HCl as confirmed by X-ray diffraction measurements, whereas silica support removal requires more aggressive HF treatment, which is likely to chemically damage the

SWNTs. The process using MgO support would therefore be scaleable for SWNT production. In this study this was preliminarily demonstrated by the production of gram quantities of highly pure SWNTs. Future work would need to focus on increasing SWNT yields and process continuity, by using a fluidized bed to facilitate point-to-point contact between gaseous precursor and catalyst particles, and admixing CO with small amounts of the more labile CH_4 precursor to enhance the kinetics of CO disproportionation.

ROLE OF CATALYST AND SUBSTRATE IN SYNTHESIS OF SINGLE WALL CARBON ANOTUBES

by
Amit Goyal

A Thesis
Submitted to the Faculty of
New Jersey Institute of Technology
in Partial Fulfillment of the Requirements for the Degree of
Master of Science in Chemical Engineering

Department of Chemical Engineering

May 2003

Blank Page

APPROVAL PAGE

ROLE OF CATALYST AND SUBSTRATE IN SYNTHESIS
OF SINGLE WALL CARBON NANOTUBES

Amit Goyal

_____

Dr. Zafar Iqbal, Thesis Advisor   Date
Research Professor of Chemistry and Environmental Science

_____

Dr. Joseph Bozzelli, Co-Advisor   Date
Distinguished Professor of Chemistry and Environmental Science

_____

Dr. Laurent Simon, Committee Member   Date
Assistant Professor of Otto York Department of Chemical Engineering

BIOGRAPHICAL SKETCH

Author: Amit Goyal

Degree: Master of Science

Date: May 2003

Undergraduate and Graduate Education:

- Master of Science in Chemical Engineering,
  New Jersey Institute of Technology, Newark, NJ, 2003

- Bachelor of Engineering in Chemical Engineering,
  Manipal Institute of Technology, Manipal, Karnataka, India, 2000

Major: Chemical Engineering

Publications:

Amit Goyal
An article, "Devil in Diesel", in the annual magazine of the Chemical Engineering Association (CHEA), 2000. On concerns of sulphur concentrations and quantities in emissions from diesel engines.

Amit Goyal, Zafar Iqbal, Wei Xu, Sheuli Zakia, Aidong Lan and Daniel L. Akins
Single-Wall Carbon Nanotubes Formed within Mesoporous MCM-41 Submitted to Journal of American Chemical Society, 2002.

This thesis is dedicated to my family
for their unending love and encouragement

ACKNOWLEDGMENT

TABLE OF CONTENTS

TABLE OF CONTENTS
(Continued)

LIST OF TABLES

LIST OF FIGURES

LIST OF FIGURES
(Continued)

CHAPTER 1

INTRODUCTION

Nanotechnology is the science and engineering of creating materials, functional structures and devices on a nanometer scale, corresponding to a length of 10^{-9} m. The fascination of downsizing materials to nanoscale dimensions comes from scientific observations of considerable change in fundamental physical, chemical and biological properties as a function of their size, shape, surface chemistry and topology. Therefore, nanotechnology has generated growing interest in the scientific community, and it has become a very active area of research.

Carbon nanotubes, which are tubular graphitic carbon nanostructures, are one of most fascinating materials for investigating nanoscale science and applications. Since, Iijima discovered carbon nanotubes in 1991 (Iijima, 1991), many research groups have extensively investigated their unique electronic and mechanical properties. Many synthetic methods, such as arc discharge (Bethune, 1993), laser vaporization (Thess, 1996) and chemical vapor deposition (Hongjie Dai, 1996), have been employed. Chemical vapor deposition (CVD) has become the method of choice with advantages such as, low cost, high purity, controlled growth, vertical alignment during growth and high yields. However, only larger diameter multiwall carbon nanotubes have been produced in high yields and desired alignments by CVD, and therefore much needs to be done in the area of scaleable production and growth of single wall carbon nanotubes (SWNTs) and SWNT architectures by this technique. Functional SWNTs, due to their molecular-scale diameters, are expected to become the materials of choice for Nanotechnology and hence large quantities of these materials would be required for

1

scientific as well as commercial investigations. The focus of this thesis is therefore on the initial steps to a scaleable, atmospheric CVD process for the production of SWNTs. It involves the further development of a process described by Lan et al (2002) following on the work of Kitiyanan et al (2000) and Hongjie Dai et al (1996).

Following this introduction, the author will discuss "Carbon Nanotubes", it's types, synthesis and growth mechanism, properties, and applications. The Third chapter will discuss nanotube characterization techniques such as Raman spectroscopy, Scanning Electron Microscopy (SEM), X-Ray Diffraction (XRD), and Transmission Electron Microscopy (TEM). The Fourth chapter will focus on the scaleable CVD synthesis of Single Wall Carbon Nanotubes (SWNT's) as a function of catalyst/support preparation, growth conditions and purification techniques. The Fifth chapter will discuss the synthesis results, and provide conclusions and suggestions for the next phase of research on this topic.

CHAPTER 2

CARBON NANOTUBES

2.1 Overview

It is the chemical genius of carbon that it can bond in different ways to create structures with entirely different properties. Diamond and graphite are the two well-known forms of crystalline carbon. Diamond has four coordinated sp^3 carbon atoms forming an extended three-dimensional network, whose motif is the chair conformation of cyclohexane. Graphite has three coordinated sp^2 carbons forming planar sheets, whose motif is the flat six-membered benzene ring. The latter sp^2 type of bonding builds a layered structure with strong in-plane bonds and weak out-of-plane bonding of the Vanderwaals type. Graphite is thus a soft material, which slides along the planes. The story of *fullerenes* and *nanotubes* belongs to the architecture of sp^2 bonded carbon and the subtlety of certain group of topological defects that can create unique, closed shell structures out of planar graphite sheets.

Graphite is the thermodynamically stable bulk phase of carbon up to very high temperature, at normal range of pressure. This is not true when there are only finite numbers of carbon atoms; it is because of the high density of dangling bonds when the size of graphite crystallites becomes smaller (say, nanosize). At small sizes, the structure does well energetically by closing onto itself and removing all the dangling bonds. Thus, with few hundred-carbon atoms, the structure formed corresponds to linear chain, rings, and closed shells. The closed shell carbon atoms with even number of atoms are called *Fullerenes*.

To form curved structures from a planar fragment of hexagonal graphite lattice, certain topological defects have to be included in the structure. To produce a convex structure, positive curvature has to be introduced into the planar hexagonal graphite lattice. Creating pentagons does this; one needs exactly 12 pentagons to provide topological curvature necessary to completely close the hexagonal lattice, which strictly follows Euler's principle. One can thus imagine that a greatly elongated fullerene can be produced with exactly 12 pentagons and millions of hexagons. This would correspond to a *Carbon Nanotube*. Iijima first observed in 1991 that nanotubes of graphite were deposited on the negative electrode during the direct current arcing of graphite for the preparations of fullerene (Iijima, 1991)
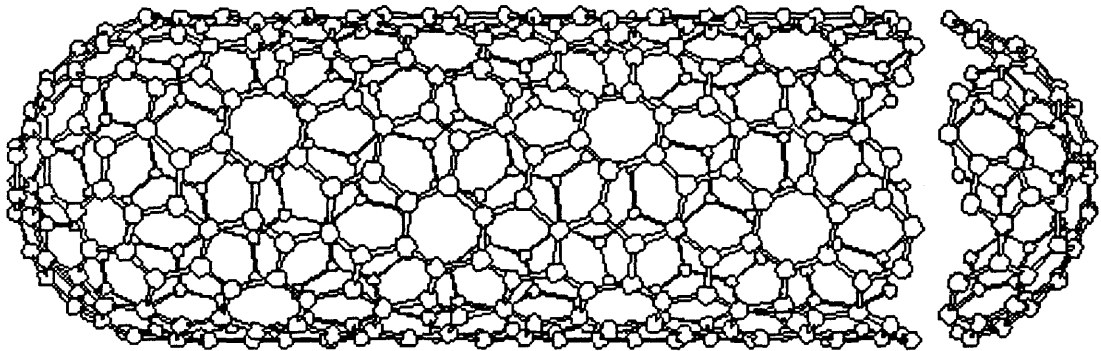
Figure 2.1 Single Wall Carbon Nanotube.

2.2 Structure and Types

An ideal carbon nanotube can be thought of as a hexagonal network of carbon atoms that has been rolled up to make a seamless cylinder. Just a nanometer across, the cylinder can be tens of microns long and each end are capped with half a fullerene molecule.

Nanotubes form in two categories. The first called multiple walled carbon nanotubes (MWNT Figure 2.2). They are made of concentric cylinders placed around a common central hollow, with spacing between the layers close to that of the interlayer distance in graphite of 0.34 nm.
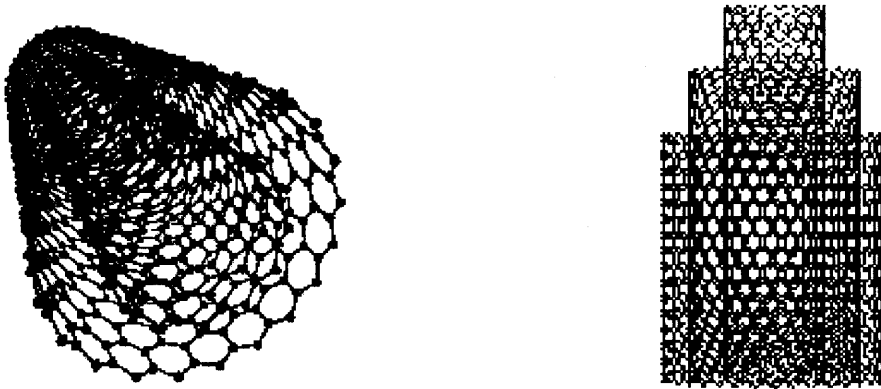
Figure 2.2 Double Wall Carbon Nanotube and Multiple Wall Carbon Nanotube.

The second are called single walled carbon nanotubes (SWNT Figure 2.1) in size they are close to fullerenes and have single layer cylinder extending from end to end. They possess good uniformity in diameter (1-2 nm)

The structure of nanotubes remains distinct from all previously known carbon fibers and filaments. As mentioned earlier, a SWNT can be thought of as a graphene sheet rolled up to from a cylinder such that open edges meet with ends closed. i.e. the pentagons are nucleated to initiate the closure mechanism. The rolling of sheet can be done in various ways, satisfying the criterion that the dangling bonds present at both the ends are matched. Any translational shift along the edges before fitting the dangling bonds will lead to a different orientation of the lattice with respect to an arbitrary tube axis. Thus, in general nanotube structure, on the curved surface of the tube, the hexagonal arrays of carbon atom wind around in a helical fashion, introducing helicity to the

structure. In the mapping of a graphene plane into a cylinder, the boundary conditions around the cylinder can be satisfied only if one of the Bravais lattice vectors (defined in term of two primitive lattice vectors and a pair of integer (m, n)) of the graphene sheet maps to a whole circumference of the cylinder. This scheme is very important in characterizing the properties of individual nanotubes as they provide the essential symmetry to the nanotube structure.
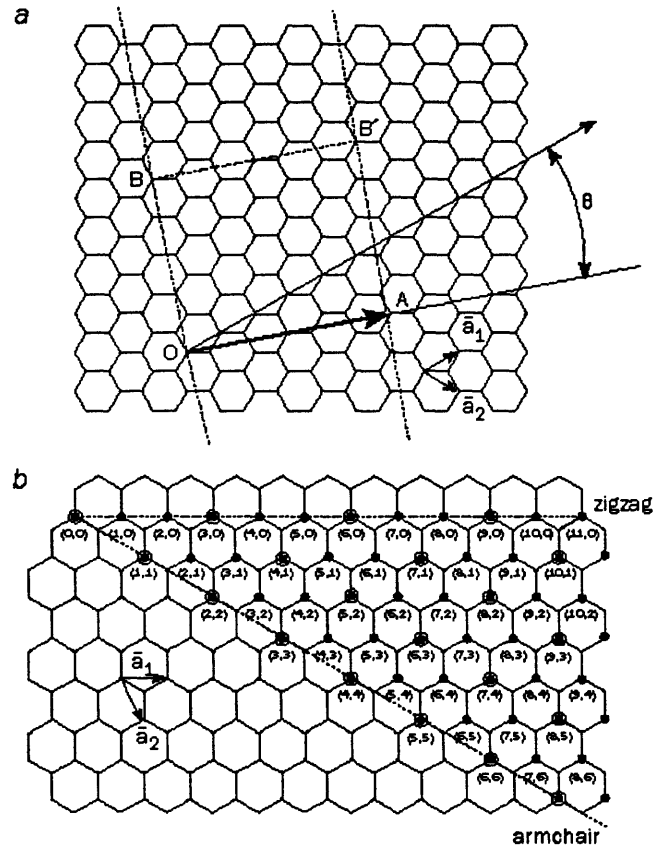
Figure 2.3 A carbon nanotube is based on a two-dimensional graphene sheet. (a) The chiral vector is defined on the hexagonal lattice as $C_h = n\bar{a}_1 + m\bar{a}_2$, where $\bar{a}_1$ and $\bar{a}_2$ are unit vectors, and n and m are integers. The unit cell of this nanotube is bounded by OAB'B. To form the nanotube, imagine that this cell is rolled up so that O meets A and B meets B', and the two ends are capped with half of a fullerene molecule. Different types of carbon nanotubes have different values of n and m. (b) Zigzag nanotubes correspond to $(n, 0)$ or $(0, m)$ and have a chiral angle of $0°$, armchair nanotubes have (n, n) and a chiral angle of $30°$, while chiral nanotubes have general (n, m) values and a chiral angle of between $0°$ and $30°$. Nanotubes can either be metallic (dots enclosed in circles) or semi-conducting (dots) (Dresselhaus, 2001).

Table 2.1 Structural Parameters for Carbon Nanotubes (Charlier, 2000)

Symbol Name	Formula	Value
"a" Length of unit vector	$a = \sqrt{3}a_{c\text{-}c} = 2.49$ A	$a_{c\text{-}c} = 1.44$ A
"$\bar{a}_1, \bar{a}_2$" unit vectors	$(\sqrt{3}/2, 1/2)\,a, (\sqrt{3}/2, 1/2)\,a$	x,y coordinate
"b_1, b_2" reciprocal lattice vectors	$(1/\sqrt{3}, 1)\,2\pi/a, (1/\sqrt{3}, 1)\,2\pi/a$	x,y coordinate
"C_h" chiral vector	$C_h = na_1 + ma_2 \equiv (n, m)$	$(0 \leq \lvert m \rvert \leq n)$
"L" length of C_h	$L = \lvert C_h \rvert = a\sqrt{(n^2 + m^2 + nm)}$	
"d_t" diameter	$d_t = L/\pi$	
"θ" chiral angle	$\sin\theta = \sqrt{3}m/(2\sqrt{(n^2 + m^2 + nm)})$ $\cos\theta = (2n + m)/\,/(2\sqrt{(n^2 + m^2 + nm)})$ $\tan\theta = \sqrt{3}m/(2n + m)$	$(0 \leq \lvert \theta \rvert \leq \pi/6)$

Nanotubes made from lattice translational indices of the form (n, 0) or (n, n) will have two helical symmetry operations while all other sets of nanotubes will have the three equivalent operations. The (n, 0) type of nanotubes are in general called *Zig-Zag* nanotubes, where as the (n, n) types are called *Armchair* nanotubes, all others are called *Helical or Chiral* nanotubes. Armchair tubes are metallic whereas zig-zag and helical tubes are either metallic or semi-conducting (Dresselhaus, 2001).
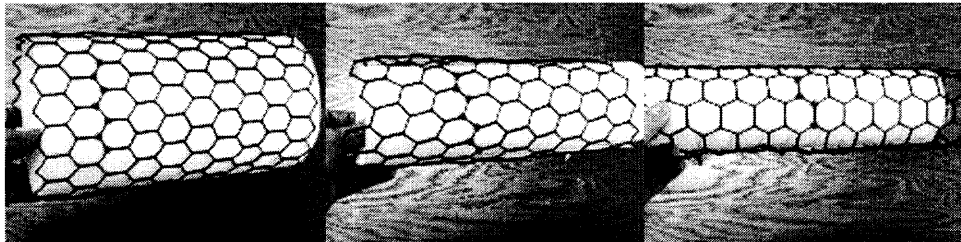
Figure 2.4 Zig-Zag Nanotube, Chiral Nanotube, Armchair Nanotube.

2.3 Methods Employed for Synthesis

2.3.1 Electric Arc Discharge Method

Nanotubes are formed in vapor, in carbon soot formed by the evaporation of modified graphite electrode i.e. anode. A hole is drilled in the anode and packed with a mixture of metal catalyst and graphite powder. When an electric arc is struck with anode, spectacular growth occurs in the reaction vessel which gets decorated with wells like structure containing SWNT's, carbon soot, catalyst particles, amorphous carbon, and fullerene molecules. The time scale for such growth is extremely small with temperature in the inter-electrode region close to 3500 C.

2.3.2 Laser Ablation

Thess, Smalley and Co-workers made high quality SWNT at 1-10g scales by this method (Thess, 1996). Intense laser pulse is used to ablate a carbon containing 0.5 atomic percent of nickel and cobalt. The target was placed in a tube furnace heated at 1200 C. During laser ablation, a flow of inert gas was passed through the growth chamber to carry the grown nanotubes downstream to be collected on a cold finger. The produced SWNT's are mostly in the form of ropes consisting of tens of individual nanotubes, closely packed into hexagonal crystals via Vander Waals interactions (Thess, 1996).

2.3.3 Chemical Vapor Deposition

In this process a catalyst material is heated to higher temperature in a tube furnace with flowing hydrocarbon gas or carbon monoxide for certain amount of time. Materials grown over the catalyst are collected after cooling the system to room temperature. The

deciding factors are choice of catalyst, carbon source, temperature window, pressure and time of growth. This process overcomes some of the problems of arc process such as fewer fullerene molecules, lower temperature and economical. It is a scaleable process and will be discussed in greater detail in chapter 4

2.4 Growth Mechanisms

Two widely acceptable mechanisms that have been for growth of nanotubes using chemical vapor deposition (CVD), "Base growth model" and "Tip growth model". In a CVD process the precursor or carbon source is catalyzed by the transition metal followed by dissolution and saturation of carbon atoms in metal catalyst particle. The precipitation of carbon from saturated metal particle leads to SP^2 structure. The tubular form is generated owing to a low energy form with no dangling bonds. In base growth model, the carbon atoms attach to the bottom of the tube with metal catalyst particle at the root. In tip growth model the carbon atom attach to the tip where metal nanoparticle is located. The whole tube structure is supported by catalyst support in both cases.

2.5 Properties

The perfect alignment of the lattice along the tube axis and the closed topology endow nanotubes with in-plane properties of graphite such as high conductivity, excellent strength and stiffness, chemical specificity and inertness together with some unusual properties such as the electronic structure which is dependent on lattice helicity and elasticity. In addition, the nano-dimensions provide a larger surface area, which could be useful in the mechanical and chemical synthesis. Both metallic and semi-conducting
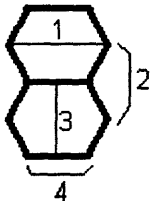
SWNT have been predicted theoretically and experimentally. The most exciting and challenging results have been transport measurements in individual nanotubes by four-probe method. Single wall Nanotube is a well-defined system in terms of electronic properties; measurements carried out in milli Kelvin range prove that SWNT can be regarded as quantum wires (Tans S.J. 1997). Unlike normal metal wires, conduction electrons in (armchair) SWNT shows an effective disorder averaged over the tube's circumference leading to electron mean free paths that increase with nanotube diameter. This increase could result in exceptional ballistic transport properties and localization lengths of several micrometers (White C.T. 1998).

Calculations suggest that nanotubes would be exceptionally stiff and strong along their length (Robertson, D.H. 1992). SWNT's with aspect ratio of the order of 1000:1 or more can be used as reinforces. Since SWNT's are made of single rolled graphene sheets, they would be ideal graphite fibers because of their elastic properties. The Young's modulous of SWNT's has been estimated on the basis of the frequency shifts of stress-sensitive Raman bands, a theoretical estimate for Young's modulus of closed SWNT's is greater that 1Tpa. Other interesting properties are listed in the following Table 2.2.

Table 2.2 Compilation of research results from scientists all over the world. All values are for Single Wall Carbon Nanotubes unless otherwise stated

Equilibrium Structure

Average Diameter of SWNT's	1.2 -1.4 nm
Distance from opposite Carbon Atoms (Line 1)	2.83 Å
Analogous Carbon Atom Separation (Line 2)	2.456 Å
Parallel Carbon Bond Separation (Line 3)	2.45 Å
Carbon Bond Length (Line 4)	1.42 Å
C - C Tight Bonding Overlap Energy	~ 2.5 eV

Group Symmetry (10, 10)	C_{5v}
Lattice: Bundles of Ropes of Nanotubes	Triangular Lattice (2D)
Lattice Constant	17 Å

Lattice Parameter:

(10, 10) Armchair	16.78 Å
(17, 0) Zigzag	16.52 Å
(12, 6) Chiral	16.52 Å

Density:

(10, 10) Armchair	1.33 g/cm^3
(17, 0) Zigzag	1.34 g/cm^3
(12, 6) Chiral	1.40 g/cm^3

Interlayer Spacing:

(n, n) Armchair	3.38 Å
(n, 0) Zigzag	3.41 Å
(2n, n) Chiral	3.39 Å

Optical Properties

Fundamental Gap:

For (n, m); n-m is divisible by 3 [Metallic]	0 eV
For (n, m); n-m is not divisible by 3 [Semi-Conducting]	~ 0.5 eV

Electrical Transport

Conductance Quantization	$(12.9 \text{ k}\Omega)^{-1}$
Resistivity	10^{-4} Ω-cm
Maximum Current Density	10^{13} A/m^2

Thermal Transport

Thermal Conductivity	~ 2000 W/m/K
Phonon Mean Free Path	~ 100 nm
Relaxation Time	~ 10^{-11} s

Elastic Behavior

Young's Modulus (SWNT)	~ 1 TPa
Young's Modulus (MWNT)	1.28 TPa

Maximum Tensile Strength   ~ 100 GPa

2.6 Applications

2.6.1 Prototype Electron Emission devices based on Carbon Nanotubes

Cathode ray lighting elements: Cathode ray lighting elements with Carbon Nanotubes materials as the Field Emitters have been fabricated by Ise Electronic Co. in Japan. Nanotube based lightning elements have a triode type design. In the early models, cylindrical rods containing MWNT's, formed as deposits by arc discharge method, were cut into thin disks and glued to stainless steel plates by silver paste, now nanotubes are screen printed to the metal plates. A Phosphor screen is printed on the inner surface of the glass plate. Different colors are obtained using different fluorescent materials. The luminescence of the phosphor screen measured on the tube axis is $6.4 * 10^4$ cd/cm^2 for green light at an anode current of 200 micro amperes which is two times more intense than conventional thermo-ionic CRT lighting elements operated under similar conditions.

Flat Panel display: Recently Samsung has fabricated a 4.5-inch diode type field emission display with SWNT stripes on the cathode and Phosphor coated ITO stripes at the anode running orthogonally on the cathode stripes. SWNT's synthesized by the arc discharge method were disposed in Isopropyl alcohol and mixed with an organic mixture of Nitro-cellulose. The paste was than squeezed into Soda lime glasses through a metal mesh, 20 micrometer in size, and the heat-treated to remove the organic binder. Y2O2 S:Eu, ZnS:Cu,Al, and ZnS:Ag,Cl, Phosphor-coated glass is used as the anode.

2.6.2 Energy Storage

Nanotube microelectrodes have been constructed using a binder and successfully used in bio-electrochemical reactions. Their performance has been found to be superior to other carbon electrodes in terms of reaction rates and reversibility (Nugent, submitted). Pure MWNT's and MWNT's deposited over catalyst (Pd, Ag, Pt) have been used to electro-catalyze oxygen reduction reactions, which are important for fuel cells.

Hydrogen storage: Materials with high Hydrogen storage capacities are desirable for energy storage applications. Metal-hydrides and cryo-adsorption are the two commonly used means to store hydrogen, typically at high pressure and or low temperature. Nanotubes have cylindrical shape, hollow geometry and nanometer-scale diameters, and can store liquid and gas in the inner cores through a capillary effect. Various amounts of Hydrogen storage density have been reported with different temperature and pressure conditions for different exposure times. The potential of achieving/exceeding 6.5-wt% storage density of hydrogen to storage system weight ratio set by Department of Energy (DOE) makes the study of SWNT a field of intense research.

2.6.3 Filled Composites

Early theoretical work and recent experiments on individual Carbon nanotubes have confirmed that nanotubes are one of the stiffest structures ever made. Theoretical studies have suggested that SWNT's could have a Young's Modulus as high as 1Tpa, which is basically the in plane value of defect free graphite. The observed tensile strength for individual MWNT's corresponds to < 60 GPa. The fractures and deformation behavior of nanotubes are intriguing; nanotubes get flattened, twisted and buckled as they deform. They sustain large strains (40%) in tension without showing signs of fracture. Such

flexibility of nanotubes under mechanical loading is important for their potential application as nanoprobes. The most important application of nanotubes based on their mechanical properties will be as reinforcements in composite materials. Although nanotube-filled polymer composites are obvious materials for applications, there have not been many successful experiments, which show advantage of using nanotubes as fillers over traditional carbon fibers. The main problem is to create a good interface between nanotubes and the polymer matrix and to attain good load transfer from the matrix to the nanotubes, during loading.

CHAPTER 3

CHARACTERIZATION TECHNIQUES

3.1 Raman Spectroscopy

Raman scattering involves an interaction between typically visible radiation with a phonon via the electronic cloud of molecules or crystals. The difference in the energy between the incoming and outgoing photons corresponds to energy of vibrations (phonons in a crystal) of the studied materials. Raman scattering follows the law of the conservation of energy and momentum. Because the momentum of the visible radiation is small, the vibrations or phonons observed by Raman spectroscopy are small and therefore lie at the Brillouin zone.

A single wall carbon nanotube can be imagined as a graphene sheet rolled into a cylinder. The reciprocal wave vector is quantized because of the periodic boundary conditions in the radial direction, leading to a confinement of electrons in this direction. This phenomenon gives rise to spikes in the density of states (DOS), called Van Hove singularities. When the energy of the incident light matches exactly the energy difference between spikes, Raman scattering becomes a resonant process. This process can occur via either the incoming or outgoing photon. Calculations have shown that the electronic transition between the Van Hove singularities depends on both the diameter and the electronic character of SWNT's. Therefore, changing the energy of the incoming photon allows to probe selectively either semiconducting or metallic SWNT's. The Raman spectrum of a SWNT is generally divided into two parts. The first corresponds to "Radial Breathing Modes" (RBM) where the frequency of vibration depends on the diameters of the SWNT's. The second corresponds to "Tangential Modes" (TM) or G bands, which

gives some insight into the electronic properties of SWNT's. Semiconducting tubes gives rise to a symmetric Lorentzian lines shape where as the metallic ones leads to Breit-Weigner-Fano resonance line shapes. This resonance is an interaction between the continuous electronic states and the discrete states of vibrations.

The main features of Raman spectra for a semiconducting tube in the TM region are a symmetrical profile with a dominant peak at around $1590cm^{-1}$ and two peaks at $1560\ cm^{-1}$ and $1550\ cm^{-1}$ often referred to as shoulder peaks. For a metallic tube, in TM, broadening of peak occurs, asymmetric band around $1540\ cm^{-1}$, a peak at $1560\ cm^{-1}$ and a sharp peak at $1580\ cm^{-1}$ is observed (Alvarez, L. 2001). In intermediate zone, several peaks are observed which are to be further investigated. One prominent broad peak cm^{-1} associated with defects on the tube walls or disordered graphite can be seen at around 1350, also called as D band.
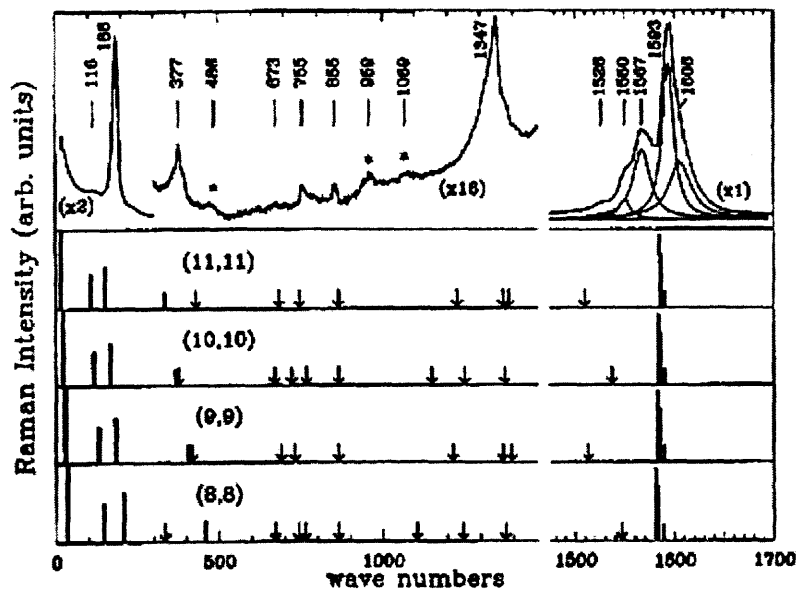
Figure 3.1 Characteristic observed (top) and calculated (bottom panels) Raman Spectra for Single wall Carbon Nanotubes (Rao, 1997).

An equation often used to calculate the diameter of a SWNT using a frequency and diameter relationship is known as Bandow eqn. (Bandow, S. 1998) as shown below.

$$\nu_{RBM} = 223.75(cm^{-1})/d(nm)$$

Where ν_{RBM} = Wavelength in radial breathing modes   (3.1)

3.2 Scanning Electron Microscopy

Scanning Electron Microscopy (SEM) is one of the most versatile techniques available for the characterization of nanotubes. The primary reason for the usefulness is the high resolution that can be obtained when bulk objects are examined. For general instruments, resolution values in the order of 2 to 5 nm are possible, while advanced research instruments have resolution less than 1 nm. One of the important features of the SEM is the three-dimensional appearance of the specimen image, a direct result of the larger depth of field, as well as the shadow relief effect of the secondary and backscattered electron contrast. In the case of carbon nanotubes, it is a good technique to check bulk yields as nanotubes form in bundles. Alignment of nanotubes can also be studied using SEM images.

3.3 X-Ray Diffraction

X-Ray diffraction (XRD) studies are done to characterize nanotubes, the XRD patterns of nanotubes show only the (hk0) and (00l) reflection but no general (hkl) reflection. Special studies have been suggested to study (hk0) reflection and it has been observed that such study support electron microscopy data (Murakami, 1993). Although in this thesis, XRD

studies were done to find the level of purity, particularly if the MgO support being used is washed away with 4M HCl after synthesis and a subsequent XRD pattern obtained is compared with the as prepared SWNT sample XRD pattern to find degree of purity.

3.4 Transmission Electron Microscopy

Transmission Electron Microscopy (TEM) is the most important technique for characterizing nanotubes. Using the high-resolution mode (0.17nm resolution used in this thesis) digital images can be captured at the atomic and molecular levels, demonstrating structural characteristics of SWNT's. One significant feature is to estimate the correct diameter and helicity of the tube, which cannot be revealed by other mentioned techniques. TEM also throws light on the qualitative details of the growth mechanism of a nanotube and packing as a bundle.

CHAPTER 4

EXPERIMENTAL WORK

4.1 Approach

To study the role of catalyst (cobalt and molybdenum) and substrates (magnesium oxide and silica opal) in synthesis of SWNT's, experiments were carried out in a horizontal CVD furnace. Different catalysts were prepared either by combustion synthesis, or on silica support by the hydrolysis of Tetraethoxysilane (TEOS). In all experiments, pure carbon monoxide was used as precursor gas, hydrogen was used as a reducing agent and cooling was done under argon atmosphere. Raman spectroscopy and SEM techniques were mainly used for characterization.

4.2 Catalyst Preparation

4.2.1 Combustion Synthesis

The catalysts were prepared by a wet mechanical mixing and combustion synthesis procedure (Patil, K.C. 1993). About 2-3 gms of Magnesium nitrate and 500 mg of citric acid were nixed. A catalyst solution of molybdenum and cobalt using ammonium molybdate and cobalt nitrate hexahydrate was made in atomic ratio of 4:1. Few drops of catalyst solution were added to a previously obtained mixture, sufficient distill water was added to obtain a clear solution. A clear pink solution resulted, the color to the solution is imparted by $Co(NO_3)_2.6H_2O$. Citric acid was used as a foaming agent. The solution was placed in a ceramic or quartz boat and covered by a flexible aluminum sheet to contain the foam generated; a tungsten wire was used to fix the aluminum sheet over boat. Boats were then introduced in a quartz tube and placed in a furnace held at 550 C for about five

19

minutes. The temperature was controlled using a programmable logic controller from Allied signals integrated with furnace. The system was allowed to cool down to room temperature under ambient conditions. Foamy material obtained was ground to a fine powder with the help of a mortar and pestle.

A different set of catalyst was made using same technique as mentioned above. In this run weighed amount of $Mg(NO_3)_2.6H_2O$ and $Co(NO_3)_2.6H_2O$, ammonium molybdate, citric acid and distill water to dissolve were mixed to obtain a catalyst in the molar ratio as $Mo_xCo_yMgO_{1-x-y}$. The most commonly used ratio was $Mo_1Co_5MgO_{94}$.

4.2.2 Catalyst on Silica Opal Support

A different support, the nanometer sized silica spheres in alcohol were prepared by the hydrolysis of tetraethoxysilane (TEOS) in a mixture of ammonium hydroxide, water and ethanol. Spherical silica particles are obtained when sufficient ammonia is present in the initial reaction mixture at room temperature. The final opal size depends mainly on the initial water and ammonia concentration. Silica powder was then obtained by evaporating the excess ethanol and ammonia. The mixture was heated at 600 C for three hours, and then particles are dispersed in ethanol again to form a suspension. The opal films are then self-assembled by laying the suspension on fused silica or quartz. The colors reflected by opal or silica spheres is due to light diffraction owing to the Bragg's law, opal samples with different diameter of 200, 245 and 300 nm scattered blue, green and red colors respectively. Such, quartz plates with thin film of opal were then deposited with few drops of molybdenum and cobalt solution in different molar ratios and were dried for a period of 24 hrs. at room temperature.

4.3 Synthesis of Single Wall Carbon Nanotubes (SWNT)

SWNT's were grown by Carbon monoxide - Chemical Vapor Deposition method (CO-CVD). Around 1-2 grams of catalyst was placed in quartz or a ceramic boat and covered using a porous Toray carbon paper to avoid loss of fine catalyst powder while vacuum is switched on. A tungsten wire was used to tie the carbon paper. The boats were placed in a three-point temperature controlled horizontal quartz tube furnace. A three-stage process namely calcination, reduction and deposition was followed in specified order. The furnace was programmed for 30 min. for first stage at a temperature of 500 C, calcination was done to get rid of acidic moisture and other volatile impurities. In second stage after pumping air, H_2 was introduced for reducing metal oxides formed for 30 min. The temperature was maintained at 500 C. and at a flow rate of 100 SCCM. Following second stage Hydrogen was pumped followed by 10 min duration for the temperature to rise to 700 C. In the final stage pure CO was introduced at a flow rate of 100 SCCM for 25 min. and the temperature was maintained at 700 C. In all the stages, pressure was maintained at 1 atm, the system was allowed to cool down under argon atmosphere to room temperature and sample collected. It should be noted that the boats and tube were thermally treated to remove carbon and other impurities deposited at 900-1000 C for 2 hrs before being reused.
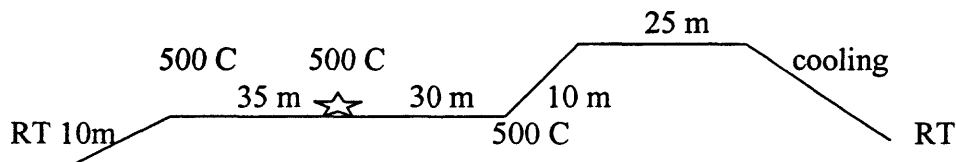
Where: m- minutes; RT- Room Temperature
Figure 4.1 Temperature program for one complete run.

4.4 Purification of SWNT

After deposition the prepared sample contains amorphous carbon, catalyst particles, support material, and SWNT's. In order to dispose of these impurities, the sample was treated with 4 M HCl to dissolve away MgO support by mechanical shaking. Following mixing ultrasonication is used for 10 to 15 minutes partially catalyst is also removed. The solution was then vacuum filtered using a teflon coated 8 μm, 47 mm filter paper and dried for a period of 24 hrs. The SWNT were then scraped from the paper and a Raman spectrum was taken to find the effect of HCl treatment. SWNT's at a concentration of 1 mg/10 ml of distill water were suspended with 1 wt % of Triton X $-$ 100 surfactant, ultrasonication was used to get a uniform suspension for about 15 minutes. Suspension was further diluted, mixed and then vacuum filtered on a teflon coated, 5 μm, 47 mm paper. It is a slow process owing to generation of foam due to surfactant. A thin black paper of SWNT results that could be peeled of from the filter paper after drying and is called a free-standing SWNT paper or a "Buckypaper". More work is needed to improve the purification stage and obtain a full sheet of free-standing paper as only bits and pieces could be peeled of owing to its brittle nature.

4.5 Chemicals and Equipment

Magnesium nitrate hexahydrate $Mg(NO_3)_2.6H_2O$ (Aldrich Chemical Company Inc.)

Cobalt nitrate hexahydrate $Co(NO_3)_2.6H_2O$ (Aldrich Chemical Company Inc.)

Ammonium heptamolybdate tetrahydrate $(NH_4)_6MoO_{24}.4H_2O$ (Aldrich Chemical Company Inc.)

Citric acid monohydrate $C_6H_8O_7.H_2O$ (Sigma chemicals)

Magnesium oxide MgO (Aldrich chemicals Company Inc.)

MTO-Triton X-100 Surfactant (Supelco)

Mass flow controllers (Sierra Instruments Inc. Range 0 – 100 SCCM)

Mass flow controller (Sierra Instruments Inc. Range 0 – 250 SCCM)

Temperature Controller (Allied-Signal Inc. corporate technology 025911)

Mechanical pump (General electric Mod: 5KC45PG1678X)

Carbon monoxide (Spectra gases)

Hydrogen (Spectra gases)

Argon (Spectra gases)

Gas Regulators (1 from Matheson gas, 2 from Prax air)

Quartz tube furnace

Quartz boats (Crown Glass Company)

Quartz tubes (Crown Glass Company)

Ceramic boats (Fisher Scientific)

Toray Carbon paper (De Nora)

Tungsten wires

Quartz plates with sputtered gold films

Raman Spectroscope (Jobin Yvon/Horiba confocal Micro Raman spectrometer)

XRD (PAN Analytial P 3040)

SEM (LEO)

TEM (JEOL 4000 EX)
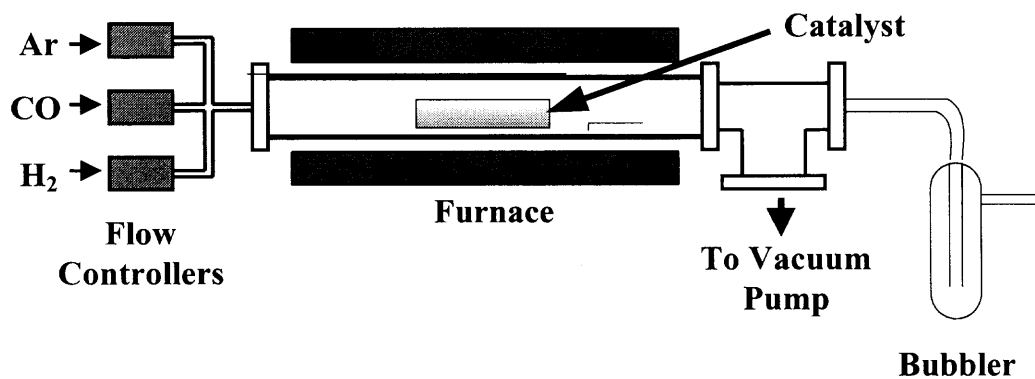
Filter paper (8 μm, 47 mm) (Whatman)

Filter paper (5 μm, 47 mm) (Whatman)

Ultrasonicator (Bransonic 521)

Pressure Gauge (Kurt J. Lesker Co. Range 0 – 1500 Torr)

4.6   Experimental Setup

Ar: Argon

CO: Carbon monoxide

H_2: Hydrogen

Figure 4.2 Experimental Setup.

CHAPTER 5

RESULTS AND DISCUSSION

5.1 Choice of Precursor and Transition Metals as Catalyst

Carbon monoxide (CO) is used in the present research as a precursor in the synthesis of SWNT's in combination with different transition metal catalysts and supports. The rationale for using transition metal as catalysts can be found in the electronic structure of CO. CO has a lone pair of electrons on carbon :C≡O: ,which is more loosely held than the lone pair associated with the more electronegative oxygen atom. Thus carbon is able to function as an electron pair donor to form a wide variety of organometallic carbonyls with transition metals. The formation of such organometallic intermediates maybe a first step in transition metal catalyzed reactions involving CO. If one looks at phase diagrams for transition metals and carbon at high temperatures, carbon has finite solubility in these metals, which leads to the formation of metal-carbon solid solutions required for the initiation of nanotube growth. Also, CO is a stable molecule and is less likely to produce amorphous carbon on disproportionation according to the reaction below at high temperatures (Dresselhaus, M.S. 2001).

CO Disproportionation Reaction (also referred to as the "Boudouard reaction")

$$2CO \underset{\text{Transition metal Catalyst}}{\Leftrightarrow} C + CO_2 \qquad \text{Eq 5.1}$$
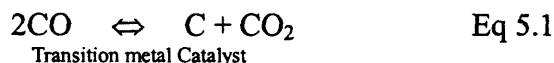
5.2 Growth Mechanism, Role of Catalyst and Support

SWNT growth occurs when carbon atoms diffuse into the interior of transition metal catalyst particles at relatively high temperatures to form a metal-carbon solid solution. Growth takes place when supersaturation leads to carbon precipitation into a crystalline tubular form. In the present study, cobalt in conjunction with molybdenum was used for the synthesis of SWNT's in different atomic weight ratios of each catalyst metal. The most successful Co:Mo ratios in terms of nanotube growth were 5:1 and 1:4, where there appears to be a window for the optimal formation of SWNTs. The distribution of SWNT diameters obtained is narrow and the tubes were found to be largely semiconducting in nature, as inferred from the Raman spectra discussed later in this chapter.

To understand the role of Mo in the synthesis, an experiment was conducted using Mo alone as catalyst. It is found that under our conditions Mo alone is inactive for SWNT growth, Though, it has been reported in the past by Dai, Smalley and coworkers that individual SWNTs can be grown at 1200 C using Mo alone as catalyst and CO as the precursor gas (Hongjie Dai, 1996). The results of Co alone as the catalyst are very interesting and discussed later in the chapter. When molybdenum is added to cobalt, it rather acts as a stabilizing agent by forming molybdenum carbide, which is a sink for active carbon species from CO disproportionation. If more carbon is deposited over the catalyst all active sites are used up and leads to either growth of multiwall carbon nanotubes or amorphous carbon. Mo helps in removing the excess carbon generated as carbide. This moves reaction 5.1 above, further to the right, thus increasing the yield of nanotubes. The yields from various runs range from 12-18%, where the %yield is defined as

%Yield = (Weight of purified sample/ Weight of as prepared sample) * 100

The two supports that have been used in the present work are polycrystalline MgO and silica in the form of three-dimensional opalic arrays. Initially, silica opal supports were used to optimize the catalyst ratio between Co and Mo in accordance with the study by Lan, Iqbal and coworkers (Lan, 2002). As mentioned in chapter 3, a thin opalic film of catalyst mixed with mono-sized silica spheres was deposited on a quartz or a silicon wafer for this kind of run, and a thin black film was formed after synthesis. Different sizes of silica spheres in the 250 to 800 nm range were used and compared after synthesis for both Co:Mo and Co alone as catalyst (Raman spectra's can be found in Appendix A). From scanning electron microscope (SEM) images (figure 5.1), it can be seen that the nanotubes grown bridge the silica spheres and are attached at both ends to a catalyst particle on each of the spheres. This technique of growing nanotubes would be extremely useful for electronic applications where patterning by lithographic techniques can be used to pre-position the catalyst particles. It is also observed that the low pressure in the deposition (third) stage of the synthesis process, i.e. when CO is introduced, is critical for the growth, this period of 2 – 3 minutes to reach atmospheric pressure always influenced the final results. It has been shown that the rate of growth of nanotubes decreases with time due to decrease in the number of available active catalytic sites (Alvarez, W.E 2001), suggesting that the first few minutes of the deposition stage are very critical. After several runs at different durations, the deposition time was optimized to 25 minutes.
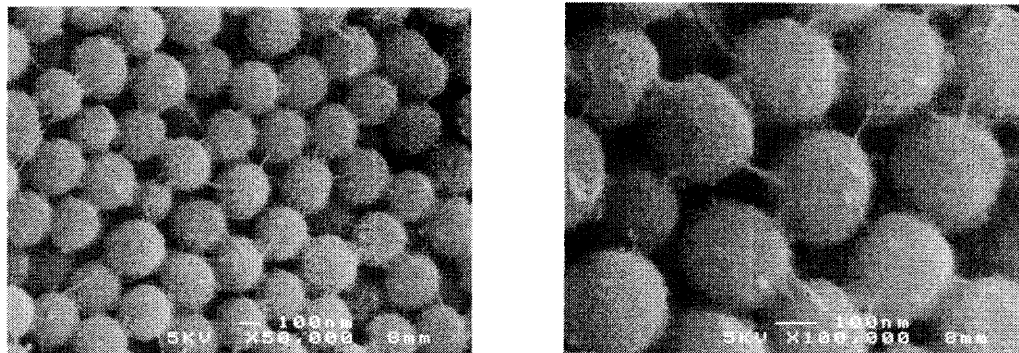
Figure 5.1 SEM images of single wall nanotubes grown within silica opal nanospheres. It can be noticed that the nanotubes bridging the silica spheres are attached to catalyst particles at both ends(Lan, 2002).

The choice of the other support studied was governed by the need to find a scaleable bulk synthesis process for SWNTs. MgO was chosen as the catalyst support because it is easily soluble in mild acids such as HCl (Li Qingwen, 2002) and HNO_3 (S. Tang, 2001). To have uniform growth, it is important to have uniform distribution of catalyst over a high surface area support. The technique used for catalyst/support preparation, i.e. combustion synthesis (Patil, K.C. 1993), helps in achieving this. The synthesis was performed using a mixture of catalyst and support compounds and citric acid to form a uniform, aqueous solution, which upon firing gave a fine creamy powder with well-distributed catalyst. Another important reason for using MgO as support is that it possesses a large number of alkaline reaction sites on which some metal oxides have been shown to be able to disperse well even at the temperatures required for nanotube growth. The growth largely occurs in bundles of individual SWNTs. This can be seen in SEM images shown in figure 5.2. The image shown on left at higher magnification is of purified SWNTs assembled as a sheet or nanopaper made using Co-Mo, 5:1 catalyst. The image on right is taken on SWNTs made using Co-Mo, 1.4 dispersed on a gold substrate.

The bundles overlap forming a spaghetti type microstructure in case of the nanopaper sample, while the sample on the gold substrate consists of more separated bundles.
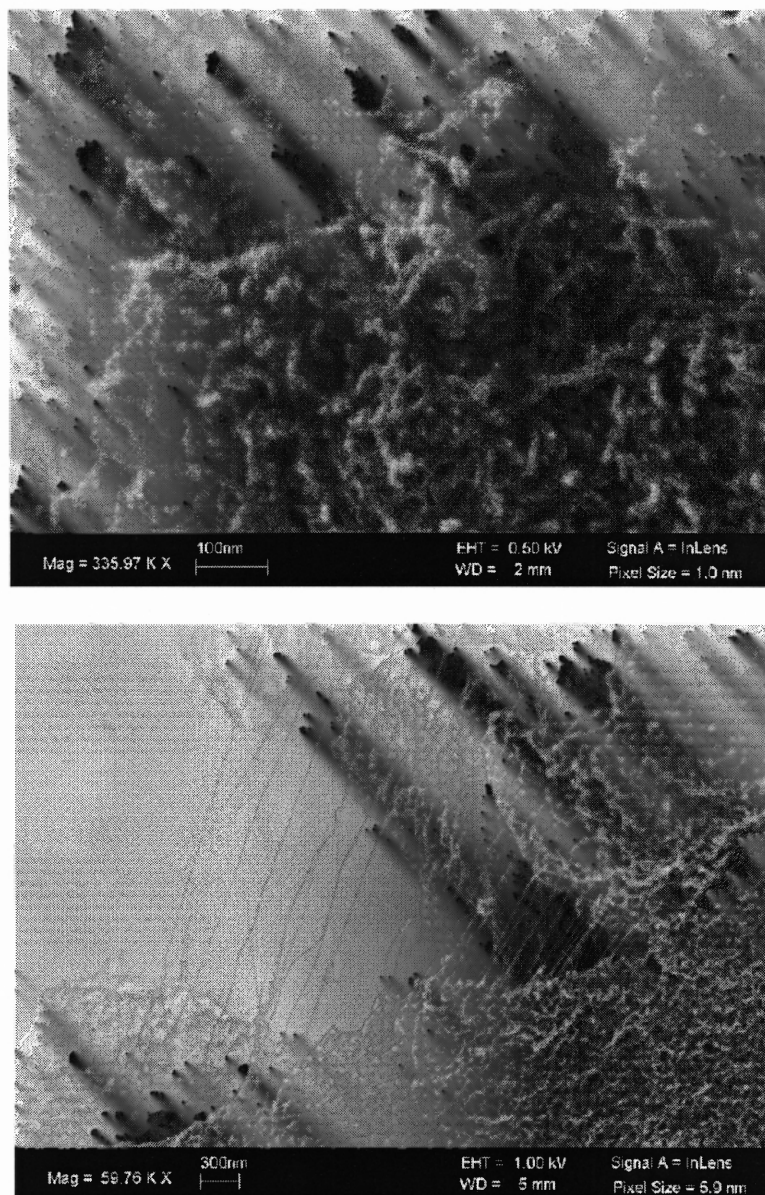
Figure 5.2 SEM images obtained from purified SWNT paper self-assembled from SWNTs synthesized using Co-Mo, 5:1 catalyst (image on top) and SWNT on a gold-coated substrate using Co-Mo, 1:4 catalyst (bottom image).

To understand the growth mechanism using this support and Co:Mo (1:4) catalyst a run was done directly on a TEM grid. In this run, the catalyst solution was mixed with acetone, after sonication a few drops of the mixture were deposited on the TEM grid and

left for drying. After synthesis, the TEM grid was examined using a JEOL 4000 EX microscope. One end of the tube is buried deep in the dark catalyst particle (figure 5.3), though it cannot be noticed whether the catalyst size is the same as the nanotube or not. The dark catalyst particle is largely covered with graphitic layers.
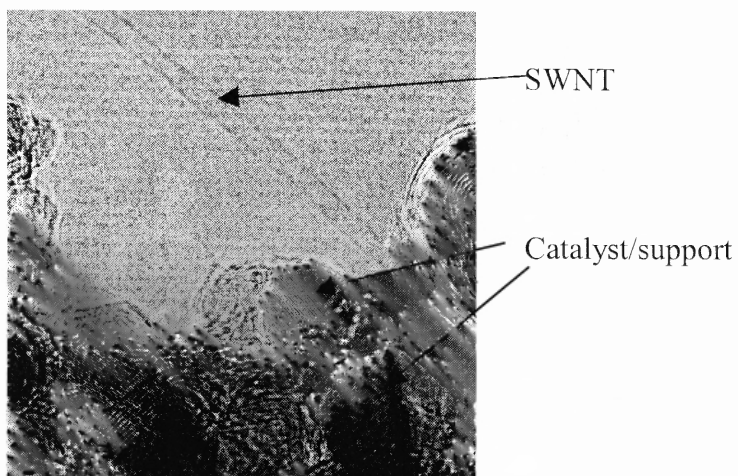
Figure 5.3 TEM image of an isolated SWNT synthesized directly on a TEM grid using Co-Mo catalyst in 1:4 ratio. The diameter of the individual tube shown here is 1.4 nm.

5.3 Analysis by Raman Spectroscopy
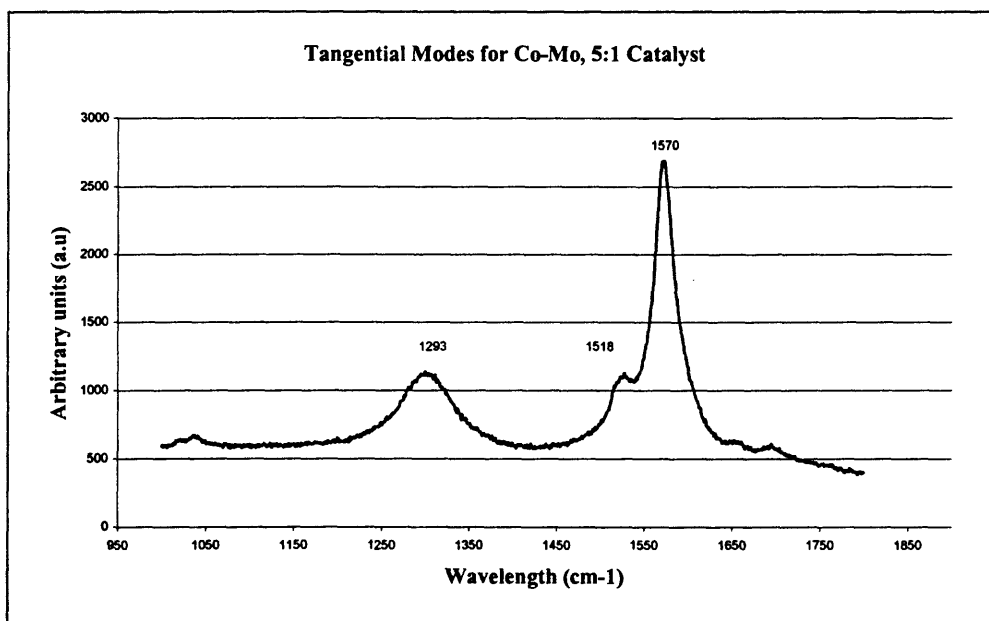
5.3.1 Co:Mo Catalyst

Raman spectra of SWNT'S prepared using different weight ratios of Co:Mo catalyst were preliminarily studied in the high frequency range using excitation laser wavelength of 488.0 nm. After confirming the characteristic peaks for single wall nanotubes, samples were studied with excitation laser wavelength of 632.8 nm using a Jobin Yvon/Horiba confocal Micro Raman spectrometer with a 50x objective lens. Largely there is no significant change in the high frequency range, i.e. of the tangential modes (TM). The Raman spectrum for an as-prepared sample using a catalyst ratio of Co to Mo of 5:1 is shown in figure 5.4 with radial breathing modes (RBM) and in figure 5.5 with tangential

modes (TM). There are two prominent peaks in RBM at 180 cm^{-1} and 267 cm^{-1} corresponding to individual SWNT diameters of 1.24 nm and 0.83 nm, (calculated using the Bandow eq., equation 3.1) respectively. In the TM region, there are three prominent peaks, first at 1293 cm^{-1} corresponding to defects on the nanotube walls. The two other characteristic peaks are at 1570 cm^{-1} and a shoulder at 1518 cm^{-1} corresponding to the tangential carbon-carbon stretching mode. The synthesis of this sample was reproducible and after purification using 1 M HCl, it was used to make a nanopaper specimen.
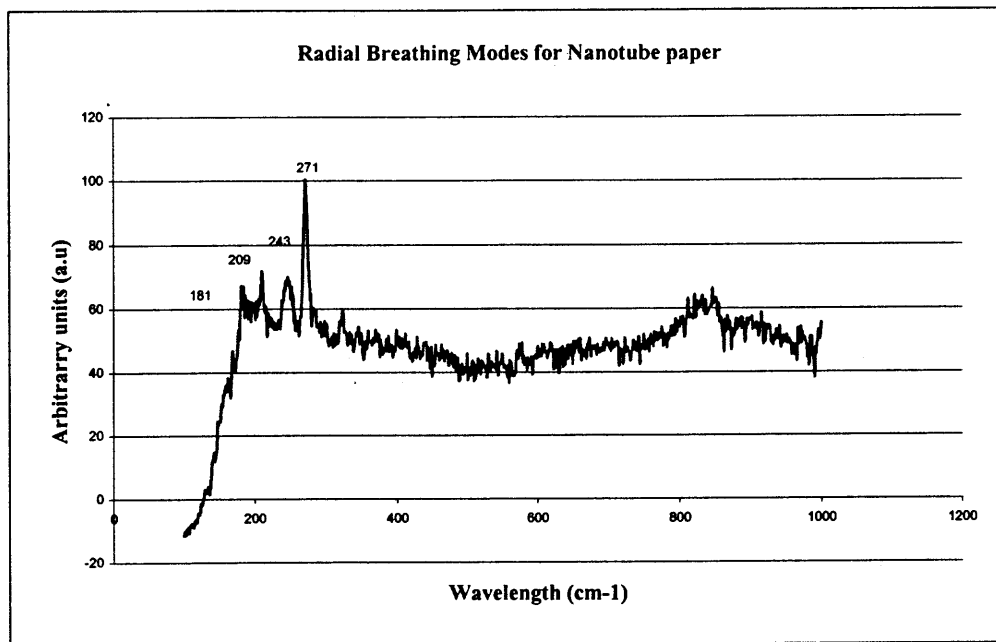
Raman spectra of the purified SWNT paper are shown in figure 5.6 (RBM) and figure 5.7 (TM). It can be noticed that there is a wider distribution of diameters, the important peaks are at 181, 209, 243 and 271 cm^{-1} corresponding to diameters of 1.24, 1.07, 0.92, and 0.82 nm, respectively. This change in diameter distribution after purification probably results from sonication (a step in the purification process), which breaks the tubes at weaker points and chops off of the hemispherical fullerene caps that usually form at the ends of the tubes, thus leaving them open-ended. In the TM region also there is a significant change showing a very sharp rise in defects on the tube walls, which could result from chemical functionalization by HCl. Another run was done to understand the purification process. The Raman spectrum of the samples prepared is shown in figure 5.8 and figure 5.9.
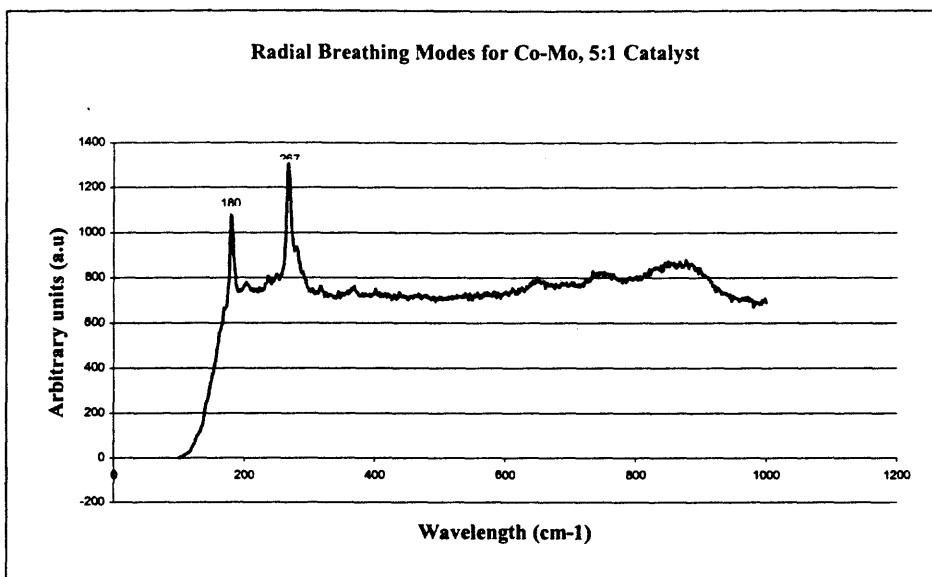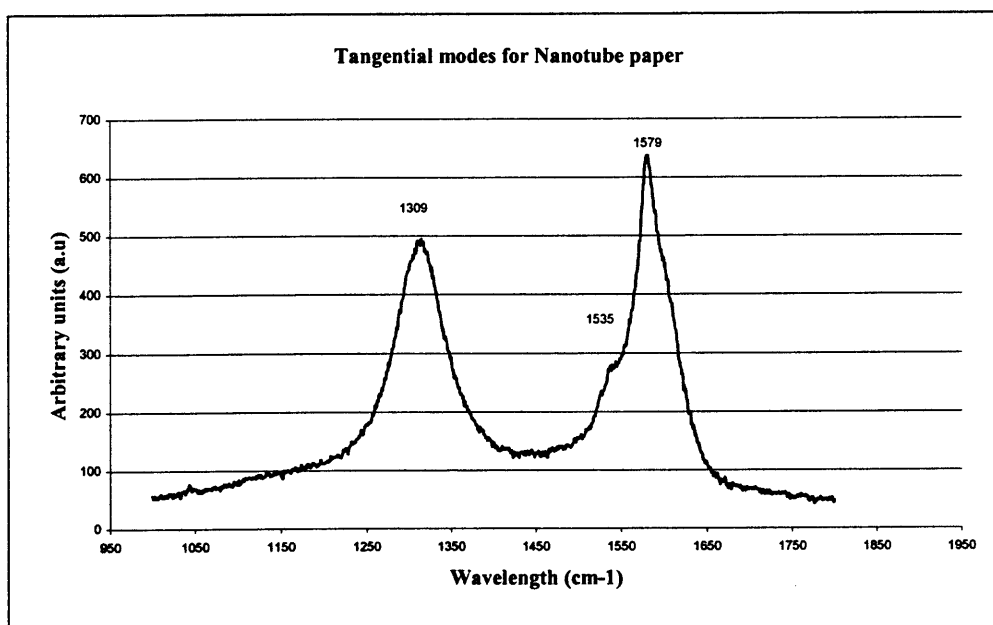
Figure 5.4 Raman spectra showing, radial breathing modes of as prepared SWNT synthesized using Co-Mo catalyst in 5:1 ratio. Exciting laser wavelength used is 632.8 nm.

Figure 5.5 Raman spectra showing tangential modes of as-prepared SWNT synthesized using Co-Mo catalyst in 5:1 ratio. Exciting laser wavelength used is 632.8nm.
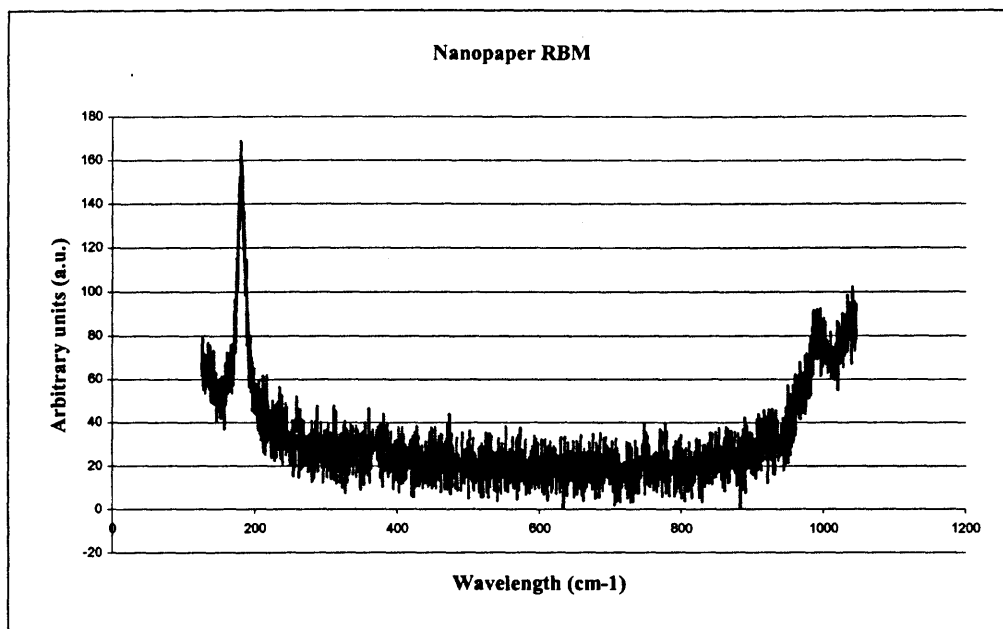
Figure 5.6 Raman spectra showing radial breathing modes of purified SWNT paper synthesized using Co-Mo catalyst in 5:1 ratio. Exciting laser wavelength used is 632.8nm
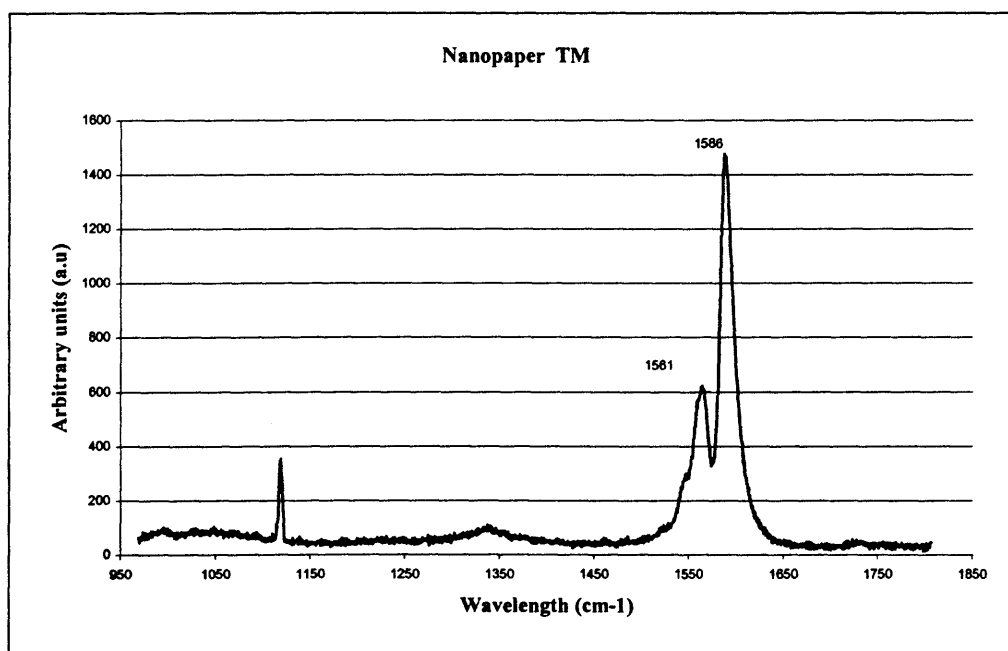

Figure 5.7 Raman spectra showing tangential modes of purified SWNT paper synthesized using Co-Mo catalyst in 5:1 ratio. Exciting laser wavelength used is 632.8nm
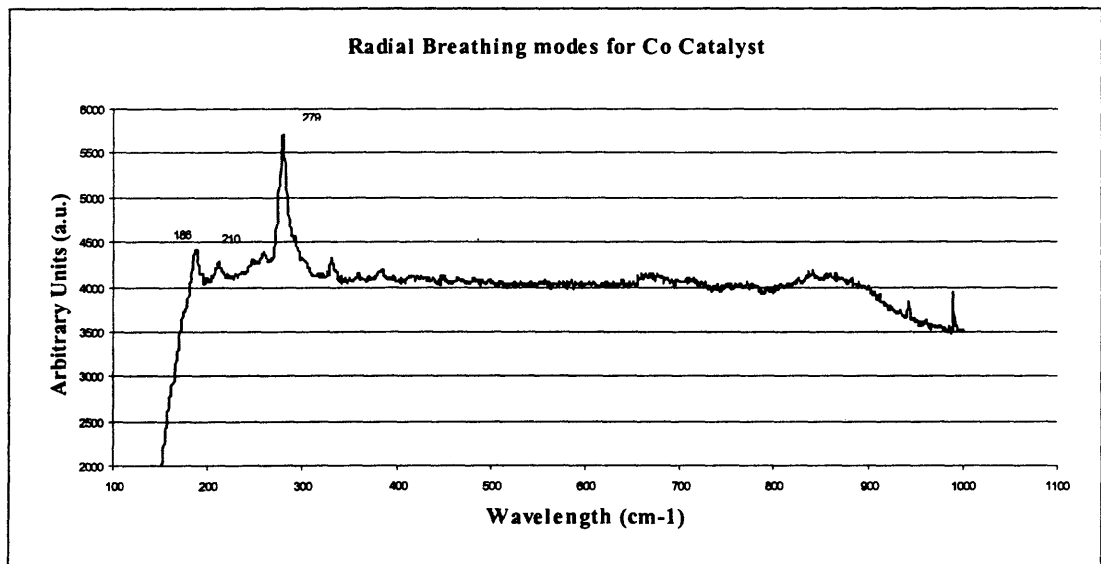
Figure 5.8 Raman spectra showing radial breathing modes of purified SWNT paper synthesized using Co-Mo catalyst in 5:1 ratio. Exciting laser wavelength used is 632.8nm.
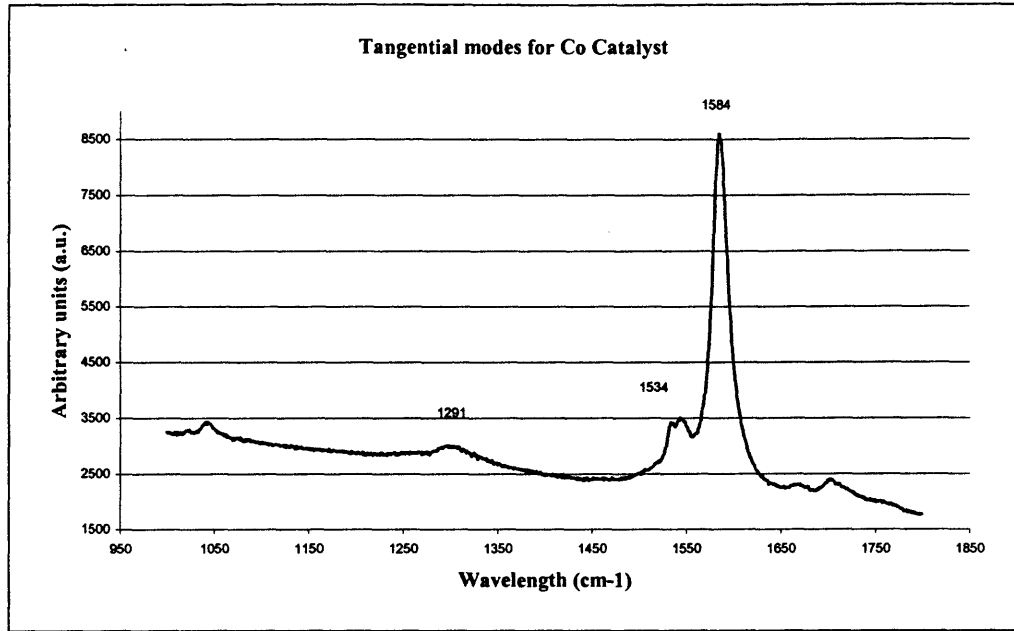

Figure 5.9 Raman spectra showing tangential modes of purified SWNT paper, synthesized using Co-Mo catalyst in 5:1 ratio. Exciting laser wavelength used is 632.8nm.
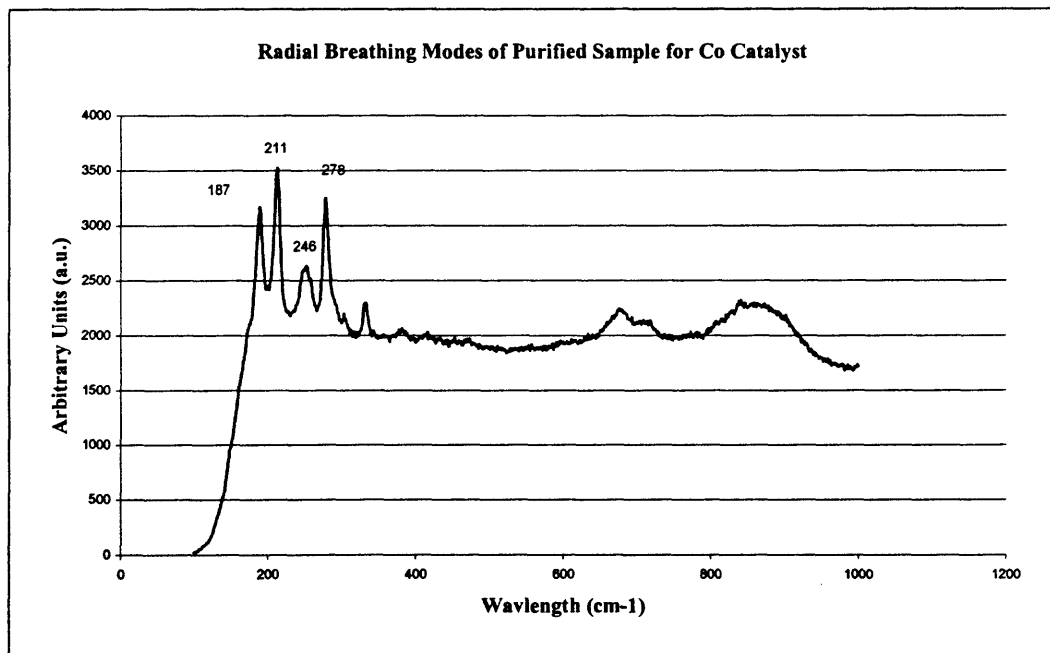
5.3.2 Co Catalyst

Contrary to the belief based on the results of different groups that it is necessary to use both cobalt and molybdenum as catalysts to grow SWNTs, we tried to use cobalt alone as a catalyst on MgO support. The results were found to be surprisingly promising, showing nanotube growth with very few defects and a similar diameter distribution as in case of the bimetallic catalyst. The advantage over the previous synthesis is in the purification stage where one has to remove fewer impurities. The synthesis with cobalt catalyst however has a lower yield as compared to the process using bimetallic catalyst, but this can probably be improved on further optimization. The Raman spectra of an as-prepared sample is shown in figure 5.10 (RBM) and figure 5.11 (TM) respectively, followed by purified samples in figure 5.12 (RBM) and figure 5.13 (TM) respectively. The spectra clearly indicate that the SWNTs prepared using Co show no change in defect concentration on purification, although there still appears to be an increase in diameter distribution.
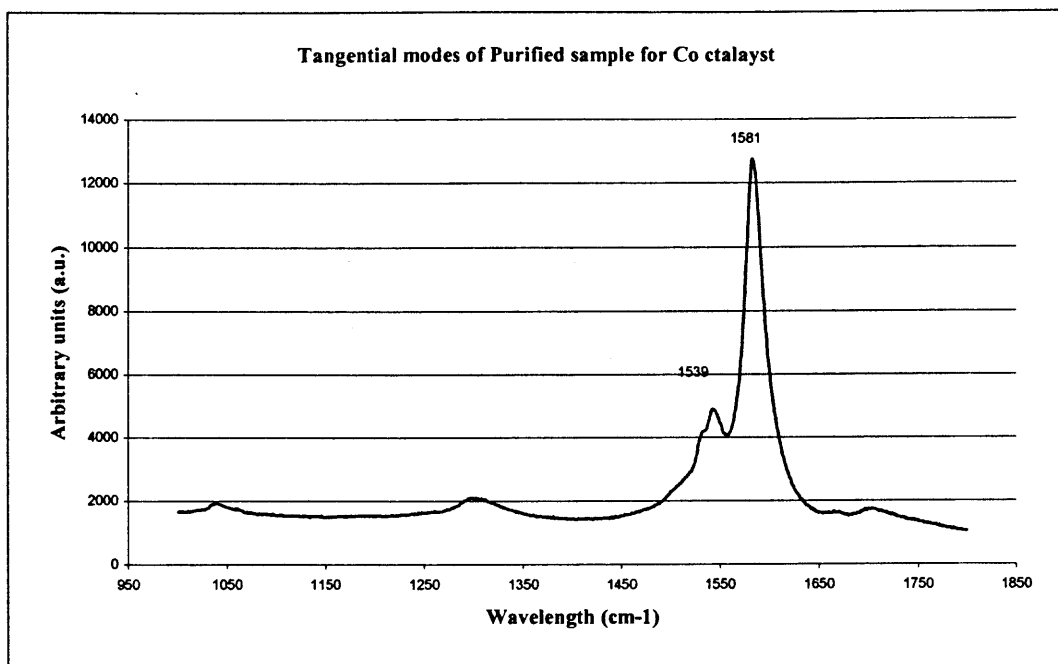

Figure 5.10 Raman spectra showing radial breathing modes of as prepared SWNT synthesized using Co catalyst. Exciting laser wavelength used is 632.8nm.

Figure 5.11 Raman spectra showing tangential modes of as prepared SWNT synthesized using Co catalyst. Exciting laser wavelength used is 632.8 nm.

Figure 5.12 Raman spectra showing radial breathing modes of purified SWNT synthesized using Co catalyst. Exciting laser wavelength used is 632.8nm.

Figure 5.13 Raman spectra showing tangential modes of purified SWNT synthesized using Co catalyst. Exciting laser wavelength used is 632.8 nm.

5.4 Analysis by XRD

In order to find the degree of purity after removal of MgO by 4 M HCl and sonication, X-Ray Diffraction patterns were obtained for catalyst, as prepared sample and for a purified sample. The diffractograms obtained are shown in figure 5.14, figure 5.15 and figure 5.16 respectively. On comparing the figures shown below it can be noticed that the patterns obtained for catalyst and as prepared sample are similar. After doing a peak search the prominent peaks shown in the figures 5.14 and 5.15 match closely with characteristic peaks for MgO. The third pattern does not show any of MgO peaks, the difference in counts is due to use of different diffraction slit widths on two occasions.
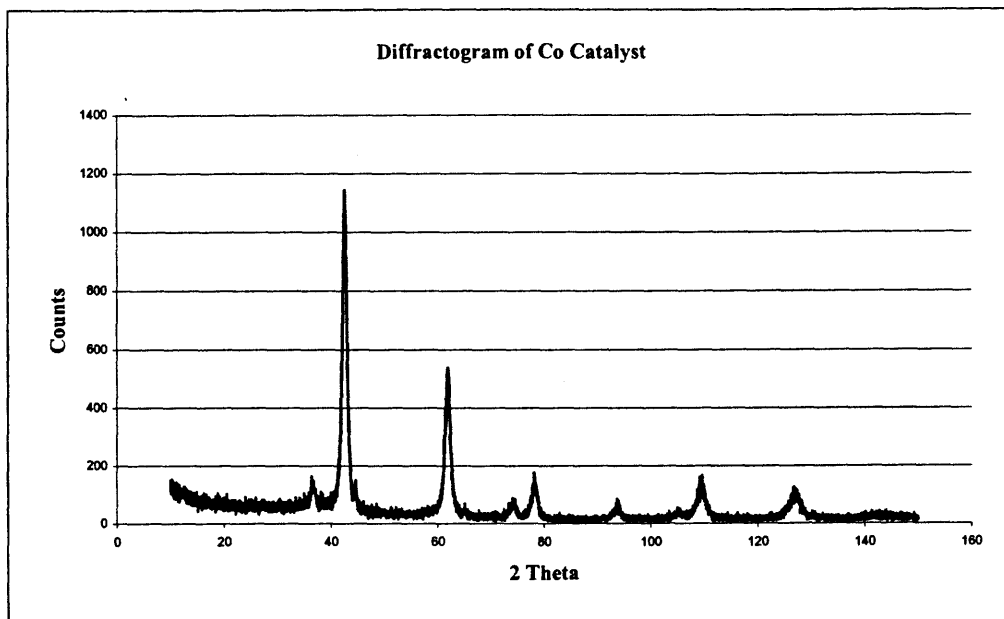
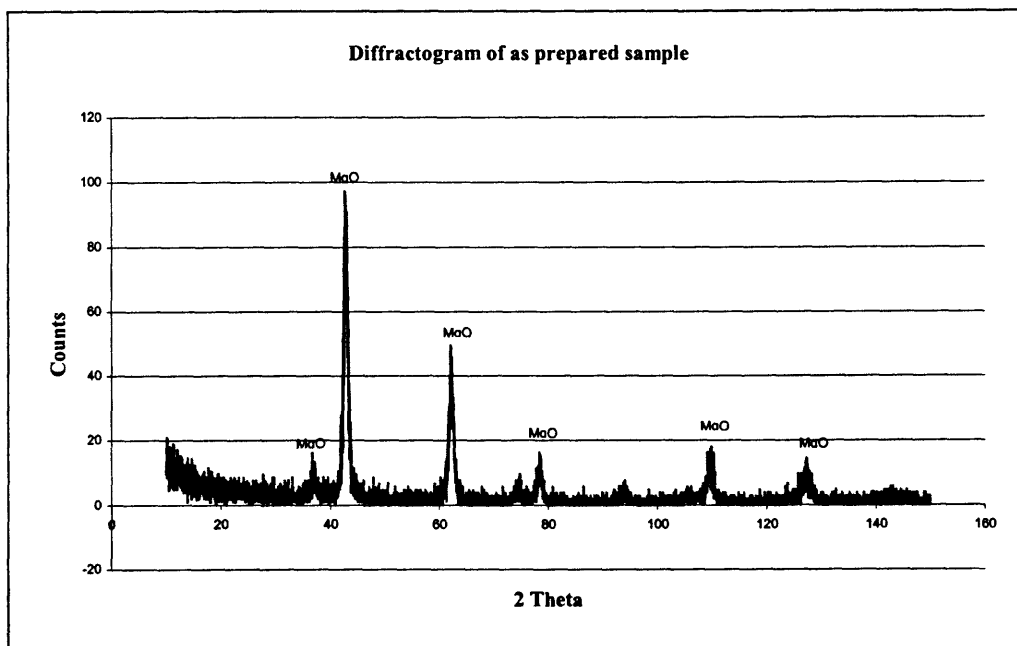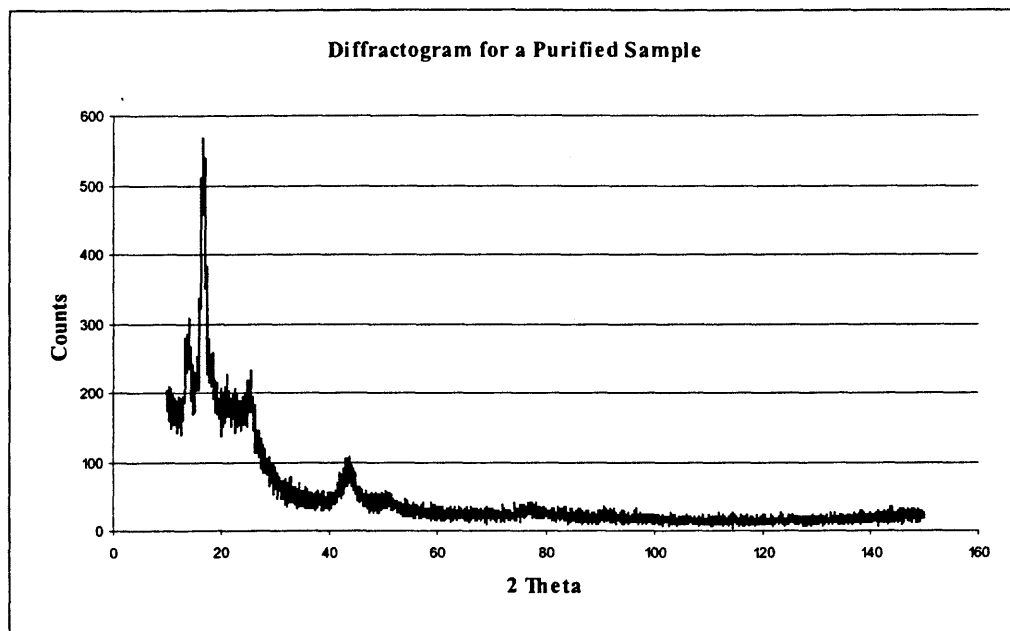**Figure 5.14** X-Ray Diffractogram for Co Catalyst with MgO as support.

Figure 5.15 X-Ray Diffractogram for as prepared sample with MgO as support.

Figure 5.16 X-Ray Diffractogram for a purified sample.

CHAPTER 6

CONCLUSIONS

Synthesis of single wall nanotubes (SWNT's) was studied using transition metal and bimetallic catalysts over two different supports. The method used for synthesis is chemical vapor deposition with carbon monoxide as precursor. Nanotubes synthesized using cobalt (Co), molybdenum (Mo) bimetallic catalysts were largely semiconducting in nature (based on the Raman data) and had a narrow diameter distribution. It is found that Co is the active catalyst and Mo acts, as a stabilizing agent. The two combinations of Co and Mo exists with both being in excess show high yields.

Synthesis using Co alone as a catalyst on silica opal support also showed good results but would need further study. Raman investigation of such samples showed very uniform growth all over the substrate. In case of bulk studies i.e. using MgO as support, yield is low and more work is needed. It is observed that MgO is an excellent support, which can be easily removed using 4M HCl as confirmed by X-Ray diffraction studies. Though it is possible that chlorine may functionalise some of the tube walls thus making it more reactive and difficult to assemble as nanopaper. It is also observed that although the catalyst level is very low, catalyst cannot be fully removed as it is attached to the roots of tubes. Two ways employed to remove catalyst were sonication and oxidation. The method results in wider diameter distribution and the second reduces the yield. Finally, synthesis of SWNT using all the above combinations of catalysts and support was highly reproducible.

CHAPTER 7

FUTURE STUDIES

The mechanisms proposed for growth of SWNT's suggest that irrespective of the methods used catalyst is an integral part of synthesis. Thus, for bulk synthesis more work is needed to optimize the size, surface area and pore volume of transition metal catalysts being used. Nanotube growth at this stage has no control, as one gets both metallic and semiconducting tube with wide diameter distribution. Both chirality and diameter are the deciding factors for all the properties of a Nanotube. There is a greater need to control the growth factors. Some work has been done in this regard by various groups including our group to grow uniform diameter tubes in Mesoporous Zeolites like MCM 41. Since SWNT's discovery in 1991 by Sumio Iijima, great theoretical work has been done in this field revealing important electronic and mechanical properties. Presently, the methods available for process are all batch processes and at lab scale further studies are needed to come up with a continuous process, like a fluidized bed catalytic reactor with catalyst regeneration to bring down the cost, which stand at a million dollar a pound hindering to harness any practical applications.
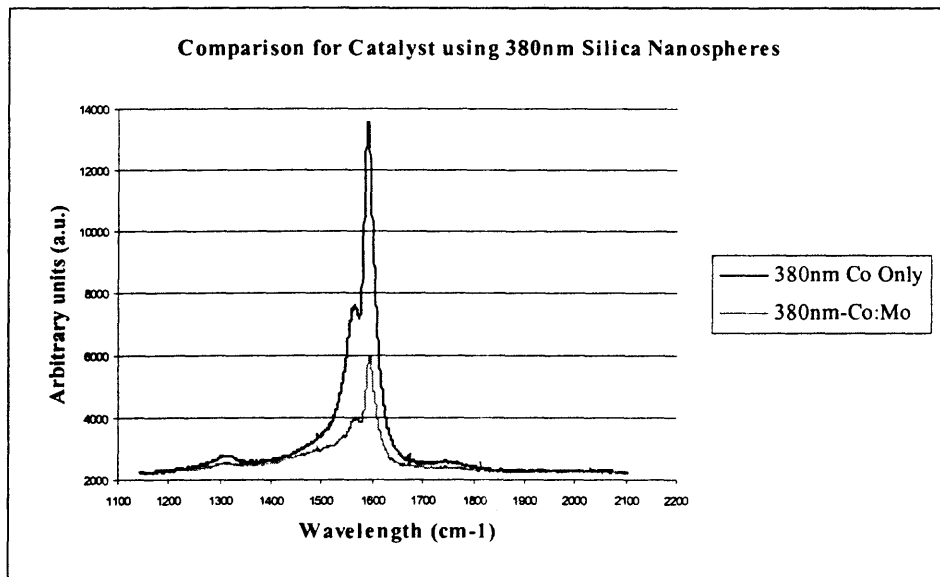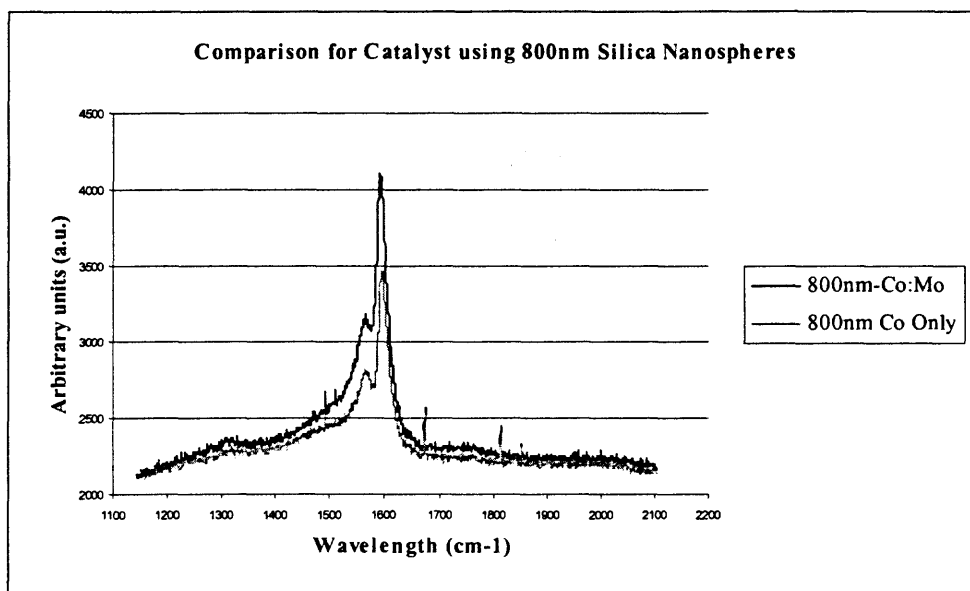
APPENDIX A

COMPARISON FOR CATALYST USING DIFFERENT OPAL SIZES
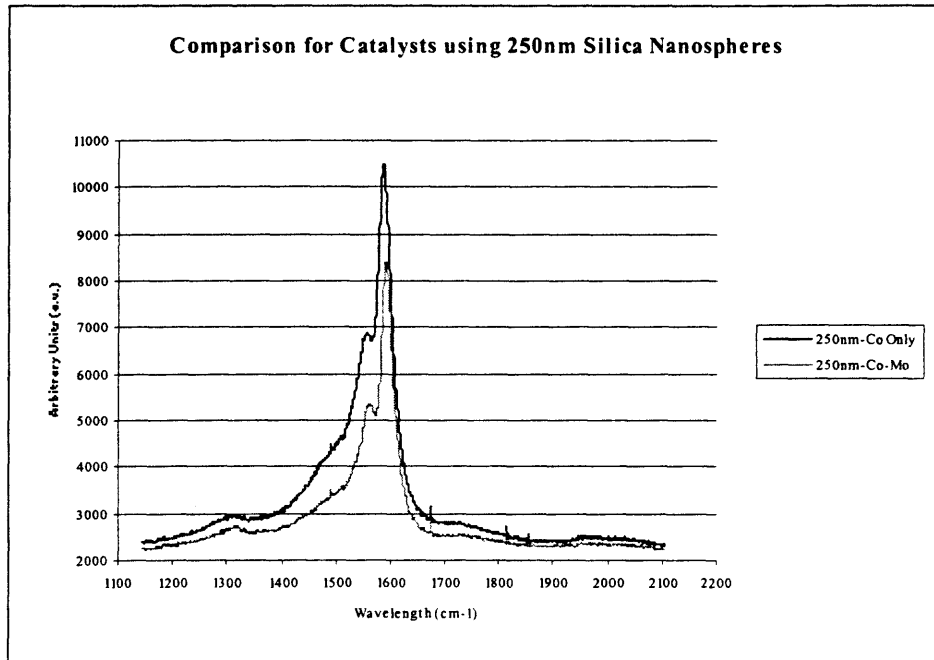
Figure A.1 Comparison for Co and Co:Mo catalyst using 250 nm Silica opal Nanospheres.

Figure A.2 Comparison for Co and Co:Mo catalyst using 380 nm Silica opal Nanospheres.

Figure A.3 Comparison for Co and Co:Mo catalyst using 800 nm Silica opal Nanospheres.

REFERENCES

Ajayan, P.M. <u>Chemical Reviews</u> 99, 1999: 1787-1799.

Alvarez, L.; Righi, A.; Rolo, S.; Anglaret, E.; Sauvajol, J.L.; Munoz, E.; Maser, W.K.; Benito, D.M.; Martinez, M.T.; and Fuente, G.F. dela. <u>Physical Review B</u>, Vol. 63, 2001: 153401.

Alvarez, W.E.; Kitiyanan, B.; Borgna, A.; Resasco, D.E. <u>Carbon,</u> 39 (2001): 547-558.

Bandow, S.; Asaka, S.; Saito, Y.; Ran, A.M.; Gregarian, L.; Richter, E.; and Eklund, P.C. <u>Phys. Review Letters</u>, 80, 1998: 3779.

Bethune, D.S.; Kiang, C.H.; Devries, M.S.; Gorman, G.; Savoy, R.; Vazquez, J.; Beyers, R. <u>Nature</u>, 363 (1993): 483.

Charlier, J.C.; Dresselhaus, M.S.; Dresselhaus, G.; Avouris, P. *Carbon Nanotubes* springer, Berlin 2000.

Dresselhaus, M.S.; Gene Dresselhaus; Avouris, Ph. *Carbon Nanotubes: Synthesis, Structure, Properties and Applications* Springer, <u>Topics in Applied Physics</u> Vol. 80, 2001.

Edelstein, A.S.; and Cammarata, R.C. 1996 *Nanomaterials: Synthesis, Properties and Applications* reprinted in 2002 by <u>Institute of Physics Publishing Ltd.</u>

Feynman, R.P. 1960 <u>Eng. Sci.</u> 2322: reprinted in 1992 <u>J. Micromech. Systems</u> ,160.

Hari Singh Nalwa, 2000 *Nanostructured Materials and Nanotechnology* reprinted in 2002 <u>Academic press.</u>

Hongjie, Dai; Andrew, G. Rinzler; Pasha, Nikolaev; Andreas,Thess; Daniel, T. Colbert; Richard, E. Smalley. <u>Chemical Physics Letters</u> 260 (1996): 471-475.

Iijima, S. <u>Nature</u> 354, 1991: 56-58.

Kitiyanan, B.; Alvarez, W.E.; Harwell, J.H.; and Resasco, D.E. <u>Chem. Phys. Lett</u> 317, (2000): 497.

Lan, A.; Iqbal, Z.; Aitouchen, A.; Libera, M.; Grebel, H. Volume 81, Number 3 <u>Applied Physics Letters</u>, 15th July 2002.

Li qingwen; Yan Hao; Cheng Yan; Zhiang Jin; and Liu Zhongfan. <u>J. Mater. Chem.</u>12, 2002: 1179-1183.

Mildred, Dresselhaus; Gene, Dresselhaus; Peter, Eklund; Riichiro, Saito. <u>Physics World</u>, January 1998.

Murakami, Y.; Shibata, T.; Okuyama, K.; Arai, T.; Suematasu, H.; Yoshida, Y. <u>J. Phys. Chem. Solids</u>, 54, 1993: 1861-1870.

Nugent, J.; Santhanam, K.S.V.; Ajayan, P.M. <u>J. Phys. Chem.</u>, Submitted.

Patil, K.C. <u>Bull. Mater. Sci.</u>, 16 (1993): 533.

Rao, A.M.; Richter, E.; Bandow, Shunji.; Chase, Bruce.; Eklund, P.C.; Williams, K.A.; Fang, S.; Subbaswamy, K.R.; Menon, M.; Thess, A.; Smalley, R.E.; Dresselhaus, G.; <u>Science</u>, Vol. 275, 10th Jan 1997: 187.

Rao, C.N.R.; Satishkumar, B.C.; Govindraj, A.; and Manasi Nath, <u>Chem. Phys. Chem.</u>, 2, 2002: 78-105.

Robertson, D.H.; Brenner, D. W.; Mintmire, J.W. <u>Phys. Rev. B</u>, 45, 1992: 12592-12595.

Tang, S.; Zhang, Z.; Xiong, Z.; Sun, L.; Liu, L.; Lin, J.; Shan, Z. X.; Tan, K. L. <u>Chemical Physics Letters</u>, 350 (2001): 19-26.

Tans, S.J.; Devrot, M.H.; Dai,H.; Thess, A.; Smalley, R.E,; Geerlings, L.J.; Dekker, C. <u>Nature</u>, 1997: 386-474.

Thess, A.; Lee, R.; Nikolaev, P.; Dai, H.J.; Petit, P.; Robert, J.; Xu, C.H.; Lee, Y.H.; Kim, S.G.; Rinzler, A.G.; Colbert, D.T.; Scuserior, G.E.; Tomanek, D.; Fischer, J.E.; Smalley, R.E. <u>Science</u>, 273, (1996): 483-487.

White, C.T.; Todorov, T.N. <u>Nature</u>, 1998: 393, 240.

Yakobson, B.I.; Smalley, R.E. <u>Am. Sci.</u>, 85 (1997): 324.